

Measurement of upper airway compliance using dynamic MRI

Yoon-Chul Kim¹, Ximing Wang², Winston Tran², Michael C.K. Khoo², and Krishna S. Nayak¹

¹Electrical Engineering, University of Southern California, Los Angeles, CA, United States, ²Biomedical Engineering, University of Southern California, Los Angeles, CA, United States

Introduction Obstructive sleep apnea (OSA) is a disease in which the upper airway (UA) narrowing/collapse induces reduction/cessation of air flow and an increased ventilatory drive leading to frequent arousals during sleep [1,2]. UA compliance, computed as the change in UA cross-sectional area per unit pressure, is a measure of airway collapsibility [3,4]. It differs between wakefulness and sleep, and is typically higher in patients with OSA compared to normals [4]. Invasive fiberoptic endoscopy has been previously used to measure the UA area and compliance [4,5]. We present an MR imaging protocol that 1) simultaneously acquires dynamic airway images and relevant physiological signals, 2) is compatible with an external airway occlusion setup, and 3) provides UA compliance measurements non-invasively.

Methods Experiments were performed on a GE Signa HDxt 3T scanner with a 6-channel carotid receive coil. Two male adults without any indications of OSA underwent MRI scans in the supine position, with airway occlusion test. The setup for airway occlusion is based on work by Colrain et al. [6].

Imaging parameters were: $16 \times 16 \text{ cm}^2$ FOV, 8 mm slice thickness, 2DFT gradient echo sequence, 100×100 matrix, 8 ms TR, 560 ms temporal resolution, 70% partial k-space, 49% gradient duty cycle. Physiological signals and images were retrospectively synchronized using timestamps. All physiological signals and MRI reconstructed frames were displayed using a custom graphical user interface in Matlab (see Figure 1).

At each time frame, the airway was segmented and UA cross-sectional areas were calculated, using Slice-O-Matic software (TomoVision, Inc.). Refer to the arrows in Fig 2b for pharyngeal airway shapes. Each UA area was normalized by the maximum UA area during tidal breathing. The normalized-area vs. pressure plot was drawn, and linear regression was performed using Matlab's *robustfit()*. UA compliance was defined as the slope of the regression (see Fig 3). Steeper slope indicates higher UA compliance and greater collapsibility.

Results The protocol supported continuous imaging of at least 30 minutes and provided image quality adequate for segmenting the airway (see Fig 2b) in all images. In both subjects, the motion/narrowing of the pharyngeal airway during occlusion was predominantly lateral (left-right) compared to anterior-posterior. Heart rate variation was correlated with the respiratory cycle, and tended to decrease during occlusion (see Fig 1). In both subjects, the UA closing pressure was less negative in the velopharyngeal slice compared to the oropharyngeal slice (see Fig 3), suggesting that the velopharyngeal site is likely to collapse first. The highest UA compliance was $0.089 \text{ cmH}_2\text{O}^{-1}$ in Subject 1 and $0.073 \text{ cmH}_2\text{O}^{-1}$ in Subject 2.

Discussion The proposed imaging protocol allows for the measurement of UA compliance during wakefulness, and is capable of scanning for several hours continuously, which will be appropriate for its measurement during natural sleep [7]. Imaging with higher temporal resolution will be desirable for the regression analysis because it enables acquisition of more sample points in the UA area change during inspiratory load. A high degree of inspiratory drive during occlusion gives larger dynamic range of sample distribution in the normalized UA area vs. mask pressure plot, and is expected to help improve accuracy in the regression analysis. Our next planned step is to measure the effect of the wakefulness and sleep state on UA compliance and compare these values between patients with OSA and age-matched controls.

Acknowledgments This work is supported by NIH Grant R01-HL105210.

References [1] Malhotra et al., *Lancet* 360:237-245 (2002). [2] Young et al., *New Eng J of Med* 328:1230-1235 (1993). [3] Ryan et al., *J Appl Physiol* 99:2440-2450 (2005). [4] Isono et al., *J Appl Physiol* 82:1319-1326 (1997). [5] Rowley et al., *J Appl Physiol* 92:2535-2541 (2002). [6] Colrain et al., *ISMRM* p2417 (2006). [7] Shin et al., *ISMRM* p4634 (2011).

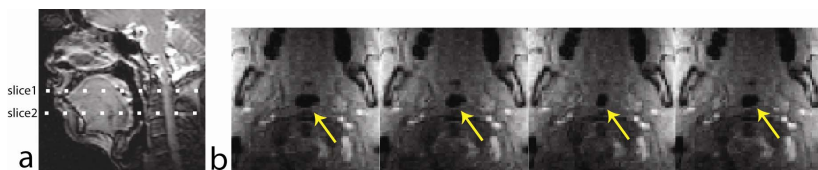


Fig 2. (a) Midsagittal image and (b) time course of the upper airway aperture (see arrows) in the velopharyngeal axial slice (i.e. slice1) during airway occlusion in the imaging of Subject 2.

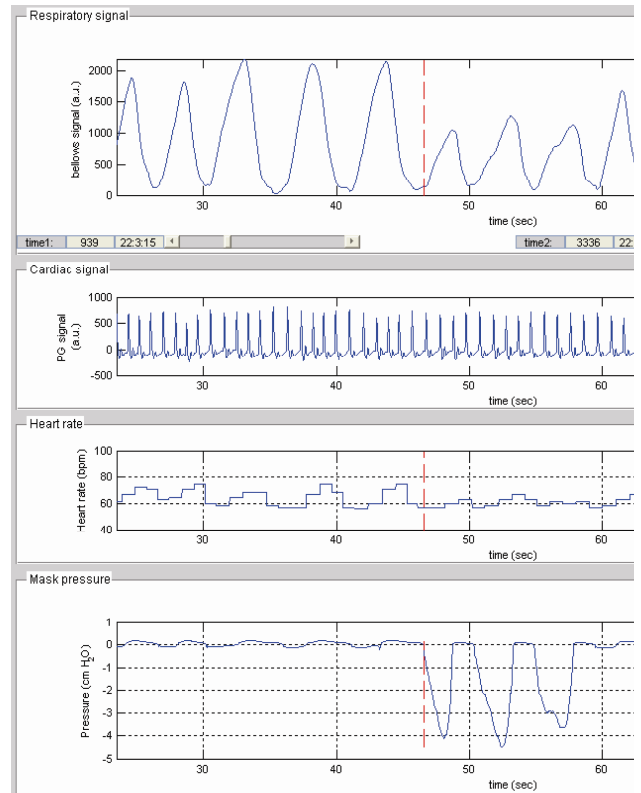


Fig 1. Physiological signals during tidal breathing and airway occlusion. The occlusion occurs at around 46 seconds. The red dashed line indicates the time corresponding to a video frame.

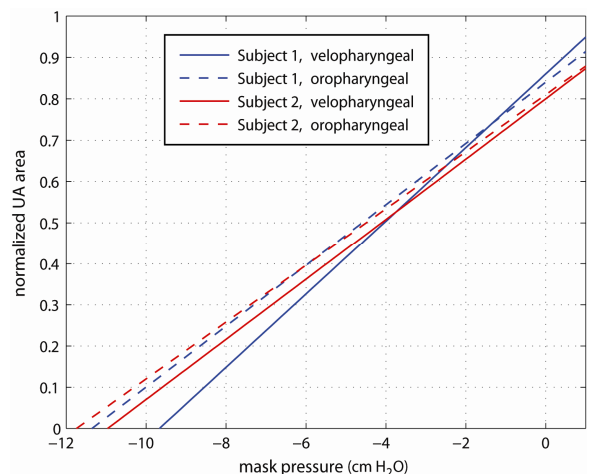


Fig 3. Linear regression plots from two subjects. The plots are obtained after regression analysis of samples corresponding to airway occlusion period.